Fuzzy Adaptive Internal Model Control Schemes for PMSM Speed-Regulation System

Shihua Li, *Senior Member, IEEE*, and Hao Gu

***Abstract*—In this paper, the speed regulation problem for permanent magnet synchronous motor (PMSM) system under vector control framework is studied. First, a speed regulation scheme based on standard internal model control (IMC) method is designed. For the speed loop, a standard internal model controller is first designed based on a first-order model of PMSM by analyzing the relationship between reference quadrature axis current and speed. For the two current loops, PI algorithms are employed respectively. Second, considering the disadvantages that the standard IMC method is sensitive to control input saturation and may lead to poor speed tracking and load disturbance rejection performances, a modified IMC scheme is developed based on a two-port IMC method, where a feedback control term is added to form a composite control structure. Third, considering the case of large variations of load inertia, two adaptive IMC schemes with two different adaptive laws are proposed. A method based on disturbance observer is adopted to identify the inertia of PMSM and its load. Then a linear adaptive law is developed by analyzing the relationship between the internal model and identified inertia. Considering the control input saturation in practical applications, a fuzzy adaptive law based IMC scheme is developed based on apriori experimental tests and experiences, where a fuzzy inferencer based supervisor is designed to automatically tune the parameter of speed controller according to the identified inertia. The effectiveness of the proposed methods have been verified by Matlab simulation and TMS320F2808 DSP experimental results.**

***Index Terms*—Adaptive control, control saturation, fuzzy inferencer, inertial identification, internal model control, PMSM.**

I. Introduction

AMONG various types of ac motors, permanent magnet synchronous motor (PMSM) has been widely used in many industrial applications due to its advantageous features such as high efficiency, high power density, torque to inertia ratio. Linear control schemes, e.g., proportional-integral (PI) control schemes, are already widely applied in PMSM systems [1]. However, PMSM servo system is a nonlinear system with multiple coupled states and parameter variations [2]. So it is very difficult for linear control algorithms to obtain a sufficiently high performance for this kind of nonlinear systems.

Manuscript received August 17, 2011; revised December 18, 2011; accepted February 22, 2012. Date of publication June 21, 2012; date of current version October 18, 2012. This work was supported by New Century Excellent Talents in University (NCET-10-0328) and National 863 Project of the Twelfth Five-Year Plan of China (2011AA04A106). Paper No. TII-11-422.

S. Li is with School of Automation, Southeast University, Nanjing 210096, China (e-mail: lsh@seu.edu.cn).

H. Gu is with Huawei Technologies Company, Ltd., Nanjing 210012, China (e-mail: guhao1985@126.com).

Digital Object Identifier 10.1109/TII.2012.2205581

Recently, with the development of modern control theory and motor control techniques, many nonlinear control methods have been reported for PMSM systems, e.g., sliding mode control [3], adaptive control [4]–[7], robust control [8], [9], fractional order control [10], disturbance rejection control [2], [11], finite-time control [12], predictive control [13], [14], and intelligent control [15], [16]. These methods not only enrich PMSM control theory, but also improve the performance of PMSM system from different aspects.

Internal model control (IMC) method was introduced by Garcia and Morari [17] and then was under intensive research and development during the past decades [18], [19]. The IMC method includes an internal model and an internal model controller which consists of the inverse internal model and a filter. It has good abilities of tracking, disturbance rejection and robustness. It also provides an effective framework for the analysis of control system performance, especially for the stability and robustness issues [17], [19]. Among these results, different kinds of modeling methods about IMC have been developed, including traditional mathematics modeling [17]–[19], neural networks modeling [20], fuzzy modeling [21], volterra series modeling [22], etc.

The internal model control method was originally applied to process control systems [18], [19] and then extended to motor control systems [23], [24]. In [23], an IMC method is applied to the current control of ac motors. In [24], an adaptive IMC method which is obtained by using Lyapunov stability theory, is proposed to control the speed of PMSM system.

It has been pointed out that although the conventional IMC method can provide an adequate suppressing ability for the disturbances added to the output channel, it may not provide a satisfactory load disturbance rejection property for the disturbances added to the input channel when the process dynamics are much slower than the desired closed loop dynamics [25]. The reason is explained and a modified design on the IMC filter is proposed for improving the performance of load disturbance rejection in [26]. Moreover, the conventional IMC control method does not consider the control input saturation in the design procedure, this may degrade the control performance and lead to windup problems [27]. Some methods have been proposed to solve this problem. In [28], an antiwindup scheme is proposed to optimize the error between the outputs of the system generated by the constrained and unconstrained control inputs. In [29], a two-port IMC control structure is proposed, where a feedback control part is added to the conventional internal model control part to form a composite controller. It is suitable for the optimum resolution of controller design trade-off between the tracking and load disturbance rejection performances.

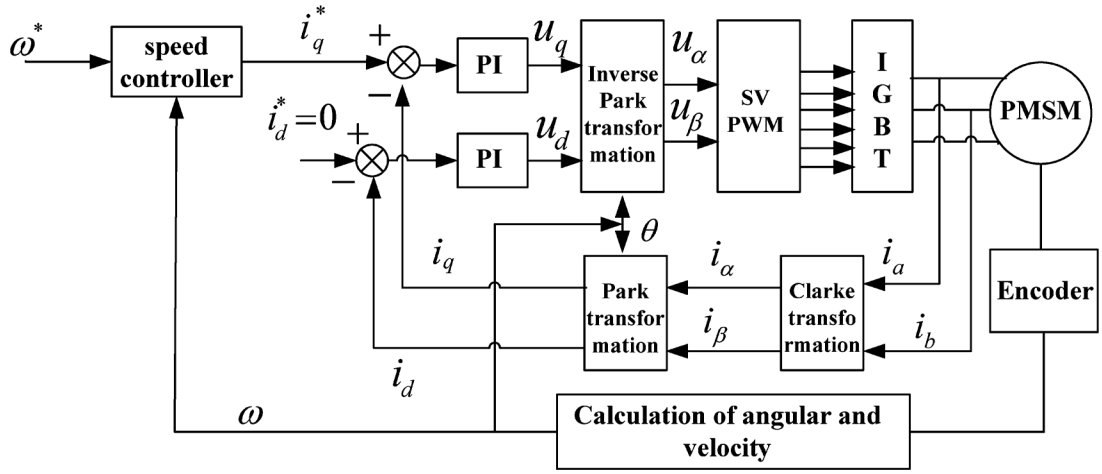

Fig. 1. Principle block diagram of PMSM speed regulation system based on vector control.

As already mentioned, the main feature of IMC is that its implementation includes an explicit internal model to be as part of the controller. However, When the mismatch between the controlled plant and internal model is large, the control performance will be diminished [30]. In some applications, e.g., electric winding machine, transfer robots with heavy loads, welding robots, etc., the inertia of the whole system increases as time goes by. When the inertia of system is increased to more than several times of the original inertia, the large mismatch between the controlled plant and internal model will cause a degradation of the closed loop performance if no corresponding control scheme is designed. In [4], by using inertia identification techniques and disturbance estimation techniques, an disturbance rejection based adaptive control scheme for PMSM speed system is presented. The feedforward compensation gain is tuned automatically corresponding to the inertia estimation value.

In this paper, different internal model control design schemes are studied for PMSM speed regulation system. First, a first order model of PMSM by analyzing the relationship between reference quadrature axis current and the speed output, and a standard internal model controller is obtained for the speed loop. For the two current loops, PI algorithms are employed, respectively. Second, considering that the standard IMC method is sensitive to control input saturation and provides a poor load disturbance rejection property, a modified IMC method proposed in [29] is introduced here and an improved IMC scheme is developed to enhance the tracking and disturbance rejection abilities. Third, further considering the case of load inertia variations, two adaptive IMC schemes are developed respectively. A torque disturbance observer (DOB) based method is employed to estimate the inertia of PMSM with load. Since the varying inertia can be estimated, the corresponding control (inertia) parameter in the internal model and the internal model controller can be linearly tuned with the change of inertia, then an adaptive IMC scheme based on linear adaptive law is developed. This method is straightforward and easy to implement. However, due to the existence of saturation, the linear adaptive law may not most suitably represent the relationship between the corresponding control (inertia) parameter and the varying inertia. Therefore, a fuzzy adaptive law is built based on apriori experimental tests and experiences to automatically tune the parameter of speed controller according to the identified inertia. Both simulation and experimental results are provided to verify the effectiveness of these IMC schemes.

II. Problem Description

In d-q coordinates, the model of the surface mounted PMSM can be described as [31]

$$\begin{pmatrix} \dot{i}_d \\ \dot{i}_q \\ \dot{\omega} \end{pmatrix} = \begin{pmatrix} -\frac{R}{L} & n_p\omega & 0 \\ n_p\omega & -\frac{R}{L} & \frac{n_pK_t}{J} \\ 0 & -\frac{n_pK_t}{L} & -\frac{B}{J} \end{pmatrix} \begin{pmatrix} i_d \\ i_q \\ \omega \end{pmatrix} + \begin{pmatrix} \frac{u_d}{L} \\ \frac{u_q}{L} \\ -\frac{T_L}{J} \end{pmatrix} \tag{1}$$

where i_d and i_q d-axis and q-axis stator currents, u_d and u_q d-axis and q-axis stator voltages, n_p number of pole pairs, R stator resistance, L stator inductance, K_t torque constant, ω angular velocity, B viscous friction coefficient, J moment of inertia, and T_L load torque.

The principle diagram of PMSM system based on vector control is shown in Fig. 1. Here, $i_d^* = 0$ strategy is used and two PI algorithms are used in the two current-loops respectively. In this paper, we concentrate on the design of speed controller.

III. Control Strategy

A. Speed Controller Design for PMSM

1) Standard Internal Model Controller for PMSM: The Standard IMC method is considered as a robust control method which includes an internal model, and an internal model controller which consists of the inverse internal model and a filter. It can guarantee the stability of system for open loop stable plants [17], [19]. The standard IMC structure for PMSM is shown in Fig. 2, where the "generalized PMSM" includes the PMSM model and the other components of the two current loops, similar to that of Fig. 1, $G_m(s)$ is the internal model, and $C_1(s)$ is the internal model controller.

From (1), we can have

$$\dot{\omega} = \frac{K_t i_q}{J} - \frac{B\omega}{J} - \frac{T_L}{J} = \frac{K_t i_q^*}{J} - \frac{B\omega}{J} - \frac{K_t d(t)}{J} \tag{2}$$

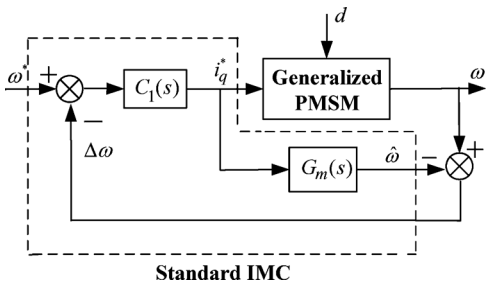

Fig. 2. Block diagram of the standard IMC method for PMSM system.

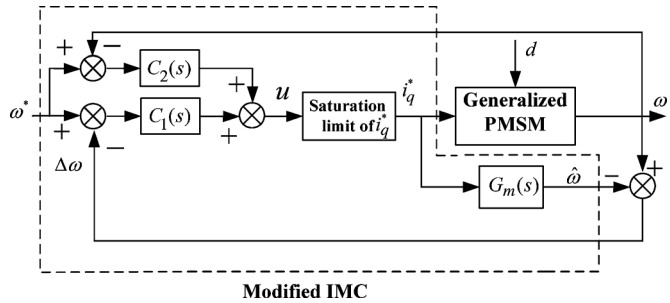

Fig. 3. Block diagram of the modified IMC method for PMSM system.

where $d(t) = -T_L/K_t - (i_q^* - i_q)$ represents the lumped disturbance, including the external load disturbance, and the tracking error of current loop of i_q.

Therefore, the generalized PMSM (the controlled model) can be described simply as

$$G_p(s) = \frac{1}{a_p s + b_p} \tag{3}$$

where $a_p = J/K_t$, $b_p = B/K_t$.

The internal model is described as

$$G_m(s) = \frac{1}{a_m s + b_m} \tag{4}$$

where a_m, b_m are the internal model parameters.

It should be noted that for the standard IMC method, if the internal model is accurate, i.e., $G_p(s) = G_m(s)$, the closed loop system is stable only if $G_p(s)$ and $C_1(s)$ are both stable [16]. In this case, the internal model controller $C_1(s)$ is defined as $G_p^{-1}(s)$, then $\omega = \omega^*$, that is the output of system attains the input of system instantaneously. But it is clear that this ideal result can not be obtained due to some reasons, e.g., $G_p^{-1}(s)$ is hardly ever proper, highly sensitive to model errors which include nonlinearity, unmodeled dynamics, and so on. Therefore, we design the internal model controller $C_1(s)$ as follows:

$$C_1(s) = G_m^{-1}(s)Q_1(s) = G_m^{-1}\frac{1}{\varepsilon s + 1} \tag{5}$$

where $Q_1(s)$ is a low-pass filter, ε is the time constant of filter.

From Fig. 2, we can obtain

$$\Omega(s) = \frac{C(s)G_p(s)}{1 + C_1(s)\left[G_p(s) - G_m(s)\right]}\Omega^*(s) - \frac{G_p(s)\left[1 - C_1(s)G_m(s)\right]}{1 + C_1(s)\left[G_p(s) - G_m(s)\right]}D(s). \tag{6}$$

If the internal model is accurate, i.e., $G_p(s) = G_m(s)$, from (5) and (6), we can obtain

$$\Omega(s) = \frac{1}{\varepsilon s + 1}\Omega^*(s) - \frac{\varepsilon s}{(a_p s + b_p)(\varepsilon s + 1)}D(s). \tag{7}$$

It can be seen from (7) that $G_p(s)$ is included in the transfer function between $\Omega(s)$ and $D(s)$ and affects the load disturbance rejection performance, no matter how the parameter ε of the IMC filter $Q_1(s)$ is tuned. Especially for a plant with a large time constant, the recovery trajectory of the load disturbance rejection may have "a long tail" [25], [26]. On the other hand, all control systems have some type of control input saturation in real applications. Although we can make the parameter ε small enough to improve the load disturbance rejection performance (e.g., less amplitude of speed fluctuation), the output of internal model controller may exceed the saturation limit of i_q^* and this will degrade the tracking performance to some extent. The reason is that if there is no model error and disturbance, the IMC system will become an open loop system. Due to control input saturation, some desired control information may lost, which may generate a short-sightedness property that can seriously degrade the performance of control system [32].

2) Modified Internal Model Controller for PMSM: In order to enhance the abilities of tracking and load disturbance rejection of the system, a feedback control term $C_2(s)$ is designed based on the standard internal model control framework. Using the two-port IMC structure in [29], a modified IMC scheme for PMSM is proposed, as shown in Fig. 3. Note that the control input u in practice usually is limited in amplitude. Thus the relationship between i_q^* and u is

$$i_q^* = \begin{cases} u, & |u| \le i_{q\max} \\ i_{q\max} \cdot \operatorname{sign}(u), & |u| > i_{q\max} \end{cases}$$

The feedback control term $C_2(s)$ is designed as a proportional term simply, which is shown as follows:

$$C_2(s) = k_p. \tag{8}$$

For the convenience of analysis, just let $i_q^* = u$, regardless of saturation. From Fig. 3, we can obtain

$$\Omega(s) = \frac{\left[C_1(s) + C_2(s)\right]G_p(s)}{1 + C_1(s)\left[G_p(s) - G_m(s)\right] + C_2(s)G_p(s)}\Omega^*(s) - \frac{G_p(s)\left[1 - C_1(s)G_m(s)\right]}{1 + C_1(s)[G_p(s) - G_m(s)] + C_2(s)G_p(s)}D(s). \tag{9}$$

If the internal model is accurate, i.e., $G_p(s) = G_m(s)$, from (5), (8), and (9), we can also obtain

$$\Omega(s) = \frac{(k_p\varepsilon + a_p)s + k_p + b_p}{(a_p s + k_p + b_p)(\varepsilon s + 1)}\Omega^*(s) - \frac{\varepsilon s}{(a_p s + b_p + k_p)(\varepsilon s + 1)}D(s). \tag{10}$$

For load disturbance rejection performance, compared with (7), it can be seen that the feedback control term k_p can be adjusted properly to reduce the time constant, i.e., $a_p/(b_p + k_p) <$

a_p/b_p, which can make the recovery trajectory in the presence of load disturbance fast to void "a long tail." Besides, when the output of the modified IMC controller is saturated, the output of the feedback control term C_2 can compensate for the effect of control input saturation as antiwindup compensation to improve the tracking performance. Through adjusting the parameter k_p properly, the closed loop system can obtain a good ability of tracking and load disturbance rejection.

3) Simulation and Experiment Results: To test the performance of the standard IMC method, simulation, and experiments on PMSM system have been performed.

The parameters of the PMSM used in the simulation and experiment are given as follows: rated speed $n_N = 3000$ rpm, rated torque $T_L = 2.4\ \mathrm{N \cdot m}$, number of pairs $n_p = 4$, stator resistance $R = 1.74\ \Omega$, stator inductances $L = 4$ mH, moment of inertia $J_n = 1.78 \times 10^{-4}\ \mathrm{kg \cdot m^2}$, torque constant $K_t = 1.608\ \mathrm{Nm/A}$, and viscous coefficient $B = 4.45 \times 10^{-4}\ \mathrm{Nms/rad}$.

Here, in the simulation, assuming that the internal model is accurate, i.e., $a_m = a_p = 6.642 \times 10^{-4}$, $b_m = b_p = 2.767 \times 10^{-4}$, we choose different values of ε to test the performance of standard IMC method. The PI parameters of both current loops are the same, where the proportional gains are 50 and integral gains are 2500. The saturation limit of q-axis reference current is ± 9.42 A.

The solid lines in Fig. 4 show the response curves of speed and i_q^* under $\varepsilon = 0.01$ where (b) is a partial enlargement graph of (a). The value of i_q^* does not exceed the saturation limit and the speed response has no overshoot and a short settling time (0.04 s). As analyzed in Section III-A1, we can reduce the value of ε to make the speed response faster theoretically. The dotted lines in Fig. 4 show the response curves of speed and i_q^* under $\varepsilon = 0.005$ without considering any saturation limit. It can been seen that at the start-up phase of motor, the maximum value of i_q^* is 14 A and the speed response has a much shorter settling time (0.02 s). However, if we consider the control saturation, things become much different. The dashed lines in Fig. 4 show the simulation results under $\varepsilon = 0.005$ with considerations on the saturation limit. It can been seen that at the start-up phase of motor, the calculation output u is over the saturation limit 9.42 A, so the value of i_q^* is cut down to 9.42 A. In such case, it can be observed that the speed response has a much longer settling time (2.6 s). These simulation results show that in the presence of control input saturation, the tracking performance of standard IMC method is degraded.

To test disturbance rejection performance of standard IMC method, a load torque $T_L = 2\ \mathrm{N \cdot m}$ is applied at $t = 15$ s. As shown in Fig. 5, the maximum amplitude of speed decrease under $\varepsilon = 0.01$ is about 174.8 rpm and the speed recovery time is 10 s. When $\varepsilon = 0.005$, the maximum amplitude of speed decrease is about 88.4 rpm and the speed recovery time is almost the same.

Here, in the experiment, the standard IMC controller parameters of speed loop are selected as: $a_m = 6.75 \times 10^{-4}$, $b_m = 2.86 \times 10^{-4}$. Then, we choose different values of ε to test the performance of standard IMC method. The parameters PI of both current loops are the same, where the proportional gains

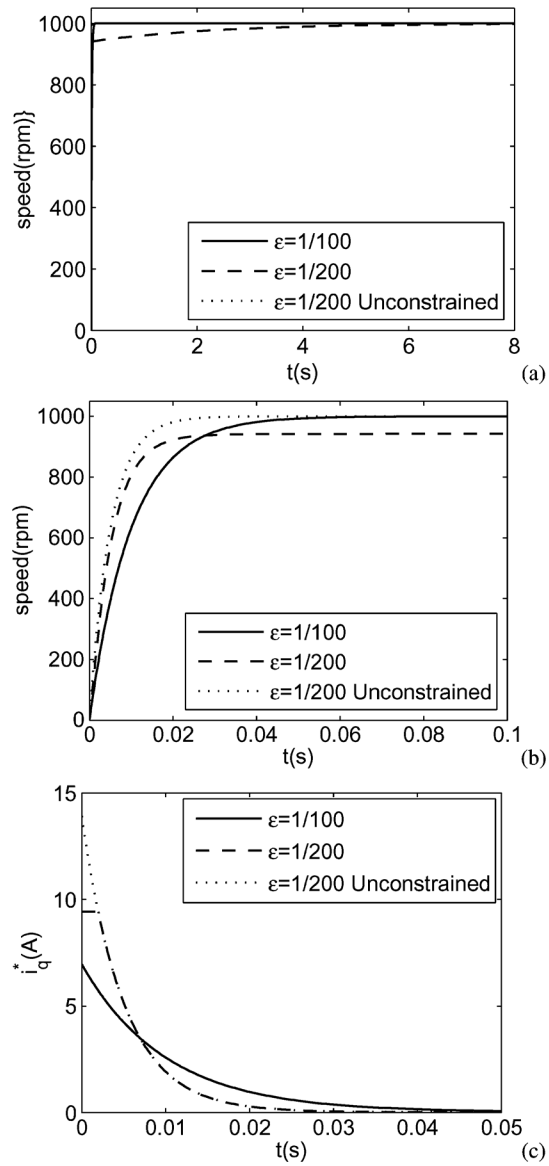

Fig. 4. Responses under standard IMC (simulation). (a) Speed. (b) Local curve of (a). (c) i_q^*.

are 42, and the integral gains are 2600. The saturation limit of the q-axis reference current is ± 9.42 A.

The solid lines in Fig. 6 show the response curves of speed and i_q^* under $\varepsilon = 0.01$. The response of i_q^* does not exceed the saturation limit and the speed response has no overshoot and a short settling time (0.22 s). The dotted lines in Fig. 6 show the experimental results under $\varepsilon = 0.005$. It can been seen that at the start-up phase of motor, the value of i_q^* is limited to 9.42 A and the speed response has a much longer settling time.

To test the load disturbance rejection performance of standard IMC method, tests have been done to evaluate the performance of PMSM system under sudden load disturbance impact, i.e., when the motor is running at the steady speed of 1000 rpm, the rated load T_L is added suddenly. As shown in Fig. 7, the maximum amplitude of speed decrease under $\varepsilon = 0.01$ is about 175.3 rpm and the speed recovery time is more than 4 s. When

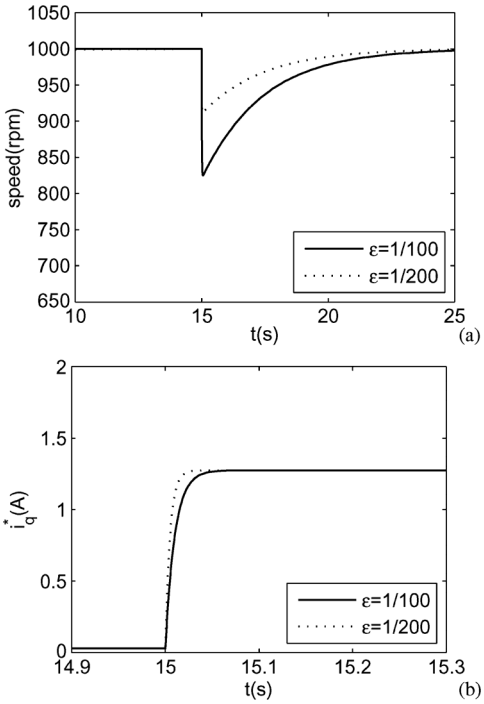

Fig. 5. Responses under standard IMC method in the presence of load torque disturbance (simulation). (a) Speed. (b) i_q^*.

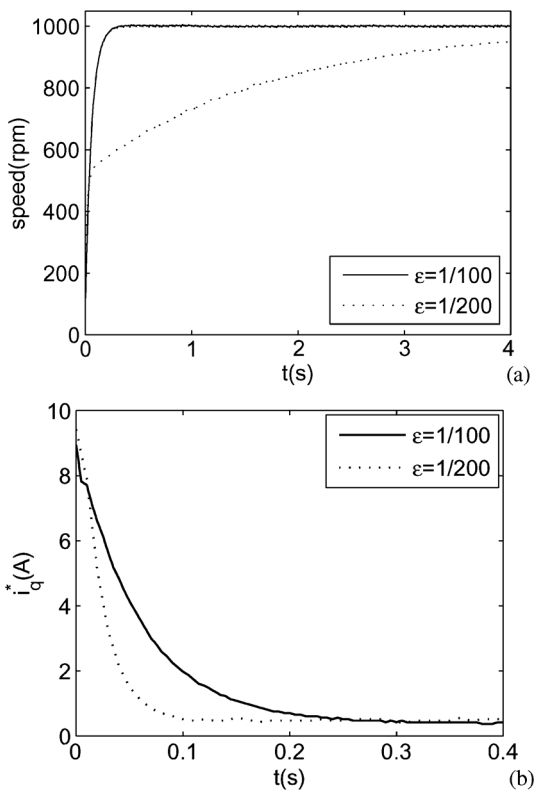

Fig. 6. Responses under standard IMC (experiment). (a) Speed. (b) i_q^*.

$\varepsilon = 0.005$, the maximum amplitude of speed decrease is about 118.5 rpm and the speed recovery time is almost the same.

From these simulation and experimental results, it can be concluded that the standard IMC method is sensitive to control input

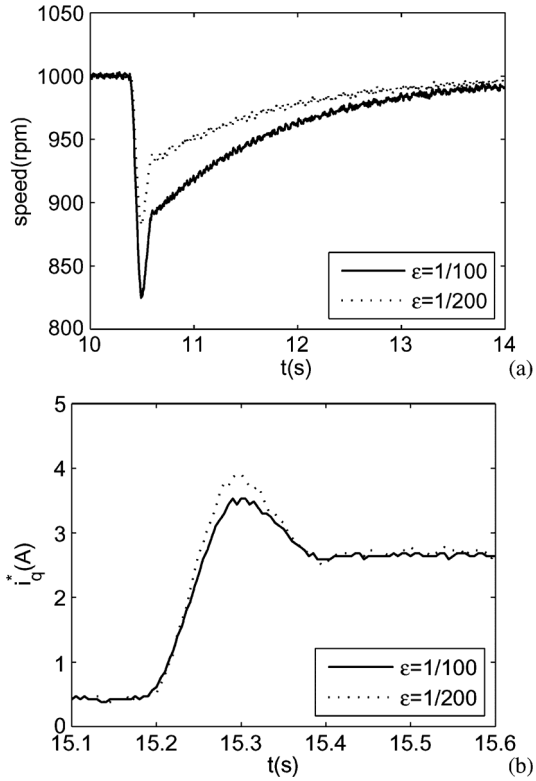

Fig. 7. Responses under standard IMC method in the presence of load torque disturbance (experiment). (a) Speed. (b) i_q^*.

saturation and may lead to poor speed tracking and load disturbance rejection performances. In order to enhance the ability of antiwindup and load disturbance rejection of the system, the modified internal model control method is applied as mentioned in Section III-A2. To show the effectiveness of the modified control method, simulation and experiments on PMSM system have been performed, which are compared with the standard IMC method.

Here, in the simulation, the controller parameters of speed loop are selected as: for the standard IMC method, $a_m = 6.642 \times 10^{-4}$, $b_m = 2.767 \times 10^{-4}$, $\varepsilon = 0.005$; the parameters of the modified IMC method are the same as the standard IMC, where $k_p = 0.1875$.

The dashed lines in Fig. 8 show the response curves of speed and i_q^* under the modified IMC. Fig. 8(b) is a partial enlargement graph of Fig. 8(a). The speed response has a small overshoot (5.12%) and a short settling time (0.021 s). The solid lines in Fig. 8 show the simulation results about the standard IMC. The speed response has no overshoot, but has a much longer settling time (2.6 s).

To compare disturbance rejection performance of both two methods, a load torque $T_L = 2\ \mathrm{N \cdot m}$ is applied at $t = 15\ \mathrm{s}$. As shown in Fig. 9, the maximum amplitude of speed decrease under the standard IMC method is about 88.4 rpm and that of the modified IMC method is much less (28 rpm). Besides this, compared with the speed recovery time under the standard IMC method (10 s), the modified IMC method has a less speed recovery time (0.05 s).

In the experiment, the speed controller parameters of the standard IMC method are selected as $a_m = 6.75 \times 10^{-4}$, $b_m =$

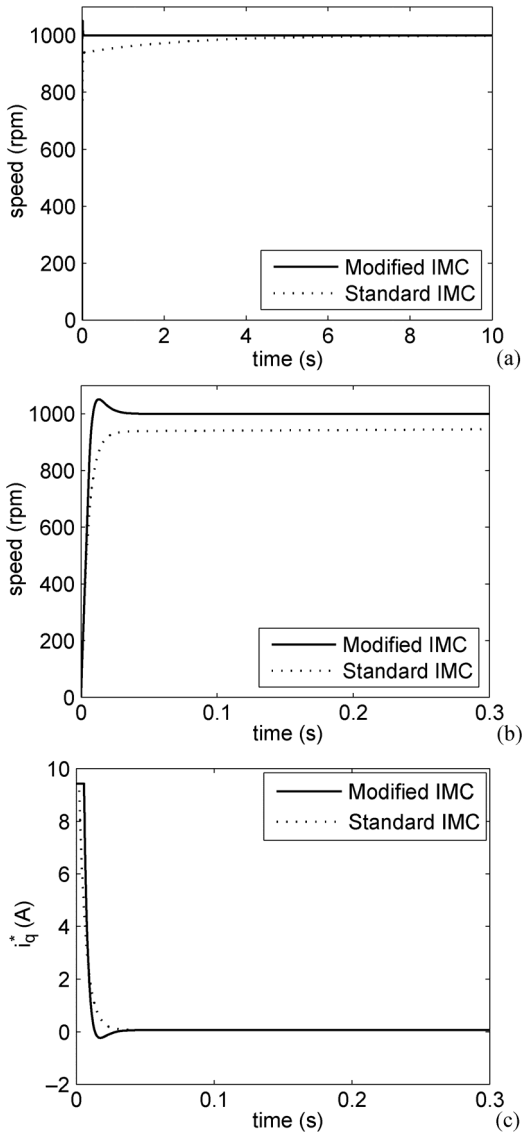

Fig. 8. Responses under standard IMC and modified IMC methods (simulation). (a) Speed. (b) Local curve of (a). (c) i_q^*.

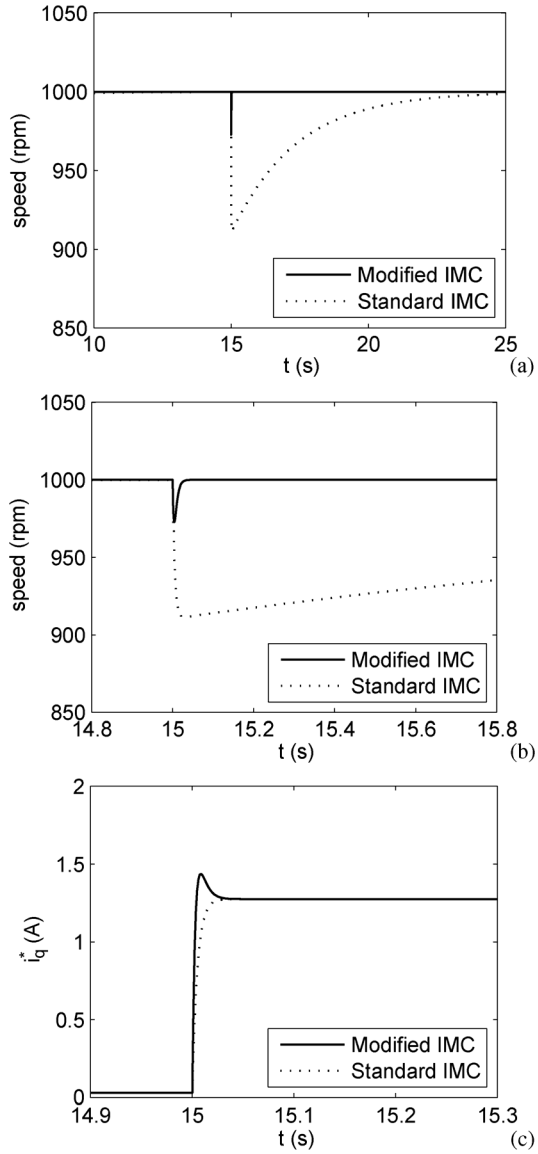

Fig. 9. Responses under standard IMC and modified IMC methods in the presence of load torque disturbance (simulation). (a) Speed. (b) Local curve of (a). (c) i_q^*.

2.86×10^{-4}, $\varepsilon = 0.005$. The parameters of the modified IMC method are the same as that of the standard IMC method except the additional parameter $k_p = 0.1875$.

Fig. 10(b) is a partial enlargement graph of Fig. 10(a). Compared with that under the standard IMC method (almost 5.5 s settling time), the speed response under the modified IMC method has a much shorter settling time (0.026 s).

To compare the load disturbance rejection performance of both methods, tests have been done to evaluate the performance of PMSM system. As shown in Fig. 11, compared with the speed decrease amplitude under the standard IMC method (118.5 rpm), the modified IMC method has a less maximum amplitude of speed decrease (21.5 rpm). Besides this, compared with the speed recovery time under the standard IMC method (more than 4 s), the modified IMC method has a less speed recovery time (0.22 s).

From these simulation and experimental results, it can be concluded that the modified IMC method has improved the tracking and load disturbance rejection performances.

B. Adaptive Internal Model Controller Design of PMSM

1) Performance Analysis: The above modified internal model control scheme for PMSM is robust to some extent. However, in practical motion control systems, there may exist cases of large variations of load inertia. For example, the inertia of electric winding machine may increase to more than several times of the original inertia. In this case, there exists a serious problem of mismatch between the internal model and the controlled plant model, which will diminish the control quality of system if the corresponding control parameters are still fixed. So for such case of parameter variations, some

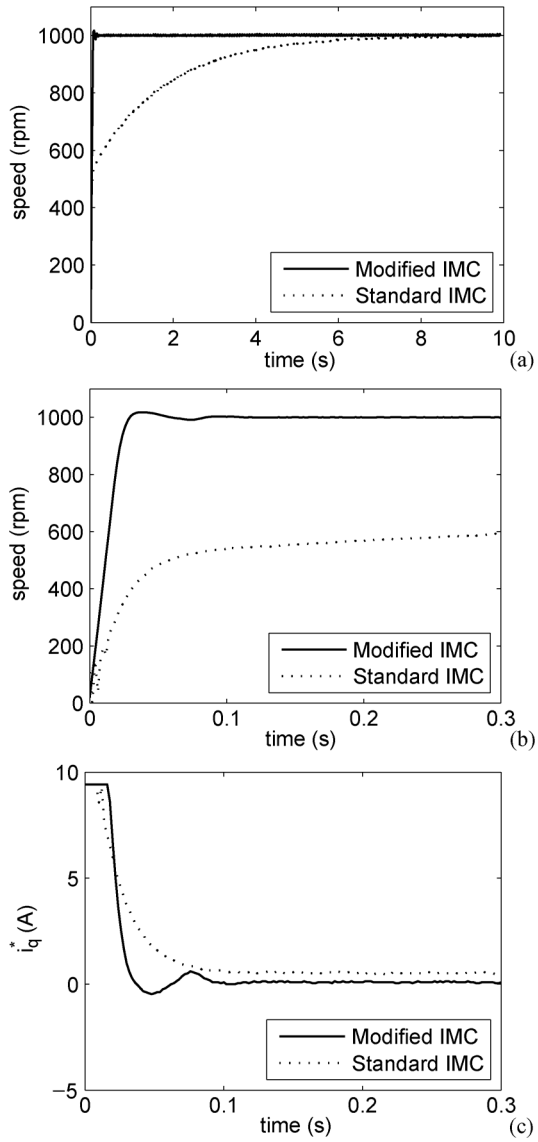

Fig. 10. Responses under standard IMC and modified IMC methods (experiment). (a) Speed. (b) Local curve of (a). (c) i_q^*.

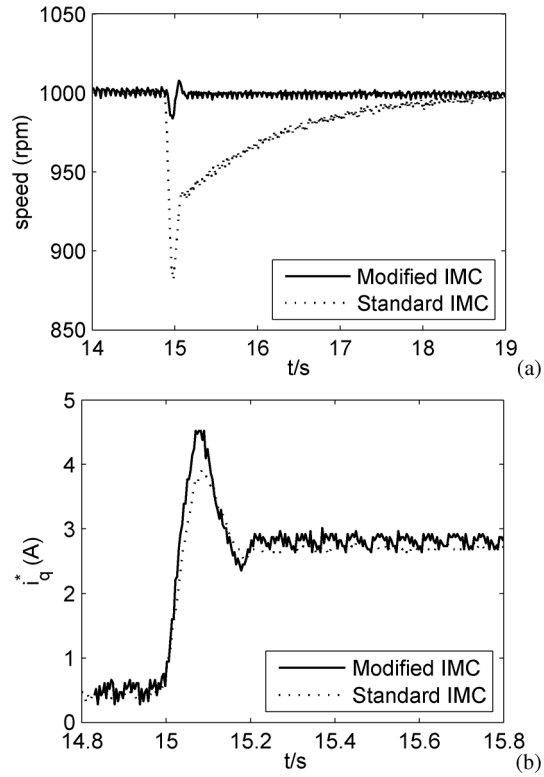

Fig. 11. Responses under standard IMC and modified IMC methods in the presence of load torque disturbance (experiment). (a) Speed. (b) i_q^*.

adequate adaptive control laws should be considered in the control design.

Next, we will show this phenomenon by simulation and experimental results. The parameters of the PMSM used in the simulation and experiment are the same as Section III-A3.

Here, at the initial stage, the motor inertia is assumed to be $J = J_n$. In the simulation, the control parameters of speed loop are selected as $a_m = J_n/K_t = 1.107 \times 10^{-4}$, $b_m = B/K_t = 2.767 \times 10^{-4}$, $\varepsilon = 0.005$, $k_p = 0.1875$.

The dashed lines in Fig. 12 show the response curves of speed and i_q^*, when the inertia of the system is J_n. The speed response has a small overshoot (6.12%) and a short settling time (0.01 s). The solid lines in Fig. 12 show the simulation results when the inertia of the system is increased to $6J_n$. The speed response has a bigger overshoot (17.81%) and a longer settling time (0.024 s). The control quality of the speed controller gets worse if the parameters of the speed controller are still fixed when the inertia of the system is increased to $6J_n$. The reason is that the parameters of the plant model is still fixed to be J_n/K_t, while it is theoretically supposed to vary with the variation of inertia.

In the experiment, the speed controller parameters of the speed loop are selected as $a_m = 1.125 \times 10^{-4}$, $b_m = 2.86 \times 10^{-4}$, $\varepsilon = 0.005$, $k_p = 0.1875$.

The dashed lines in Fig. 13 show the response curves of speed and i_q^*, when the inertia of the system is J_n. The speed response has a small overshoot (10.1%) and a short settling time (0.011 s). The solid lines in Fig. 13 show the experimental results when the inertia of the system is increased to $6J_n$. The speed response has a bigger overshoot (18.1%) and a longer settling time (0.09 s). According to the simulation and experimental results, we can see that as the inertia of the whole system varies largely, the control performance of the closed loop system will get worse if the parameters of the speed controller are not adjusted accordingly.

2) Adaptive Internal Model Control Design: For the inertia variation case, to ensure the adaptation ability of closed loop system, it is expected that if the inertia varies, the internal model and the control parameters based on the internal model can be intelligently changed. Thus, an adaptive IMC control scheme can be developed.

The block diagram of adaptive IMC scheme for PMSM speed regulation system is shown in Fig. 14, where (a) shows the whole block diagram and (b) shows the detail diagram of adaptive IMC design. A parameter autotuning strategy is adopted to tune the parameter $\hat{a}_m$ by using the estimated inertia $\hat{J}_m$.

The expression of adaptive internal model controller is as follows:

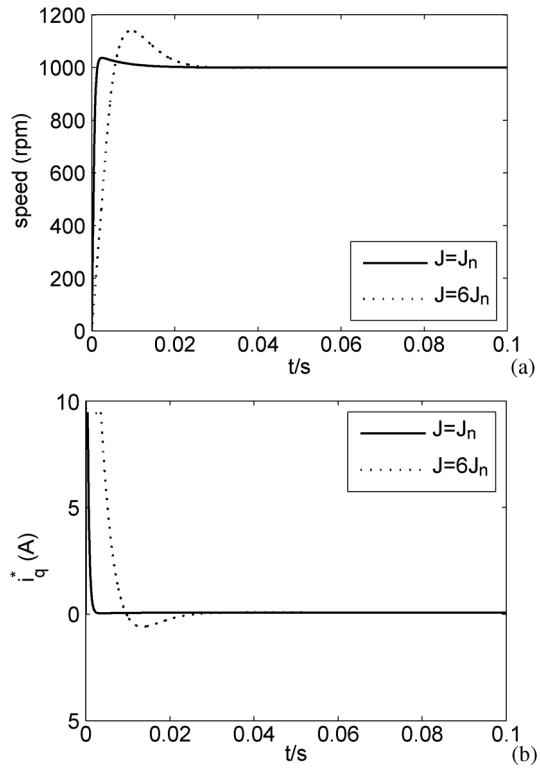

Fig. 12. Responses in the case of $J = J_n$ and $J = 6J_n$ (simulation). (a) Speed. (b) i_q^*.

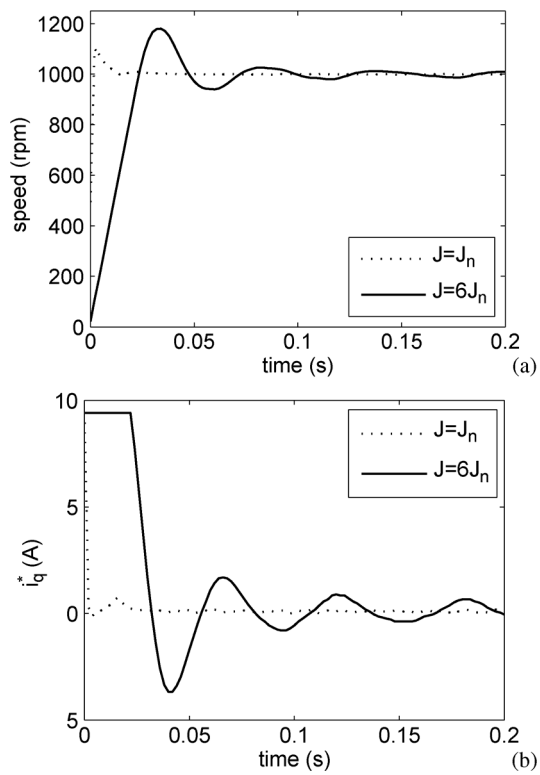

Fig. 13. Responses in the case of $J = J_n$ and $J = 6J_n$ (experiment). (a) Speed. (b) i_q^*.

1) The internal model

$$\hat{G}_m(s) = \frac{1}{\hat{a}_m s + b_m}. \tag{11}$$

2) Internal model controller

$$C_1(s) = \hat{G}_m^{-1}(s) Q_1(s) \tag{12}$$

where $\hat{a}_m$ can be tuned according to the identified inertia.

C. Inertia Identification

In this paper, we adopt the method based on DOB to identify inertia. The method estimates the external disturbances and friction in the model by disturbance estimators and then obtain an estimate of inertia [6], [33], [34]. The detailed process of this method can be found in [33], which is omitted here. The effectiveness of the method is verified by experimental results.

In this method, a test signal for inertia identification is the periodic speed command that satisfies

$$\omega^*(t+T) = \omega^*(t)$$

where T is the period of speed command.

D. Adaptive Laws

1) Linear Adaptive Law: When inertia varies, we can tune the parameter $\hat{a}_m$ of the speed controller by the estimation of inertia. To ensure the performance of the system, a linear relationship between $\hat{a}_m$ and J is established, e.g., $\hat{a}_m = J/K_t$. We can obtain the ratio of the actual inertia to the original inertia $\delta = \hat{J}/J_n$ by the estimation of inertia. The final parameter can be expressed as follows:

$$\hat{a}_m = \delta a_m. \tag{13}$$

2) Fuzzy Adaptive Law: $\hat{a}_m$ is theoretically supposed to be linearly tuned with the change of inertia, i.e., $\hat{a}_m = J/K_t$. However, in practical applications, due to the existence of control input saturation, the linear adaptive law may not be the most adequate solution.

To obtain a better performance of the system, a practical relationship between $\hat{a}_m$ and J should be established. Some apriori experimental tests should be done to help to decide the tuning expression for the parameter $\hat{a}_m$. So the internal model controller $C_1(s)$ and the internal model $G_m(s)$ both are adjusted properly according to the parameter $\hat{a}_m$, which is consistent with internal model design method [17], [19].

To this end, a fuzzy inference engine [35], [36] is chosen to describe the autotuning function for the parameter $\hat{a}_m$. The fuzzy implement is the one-input-one-output case. By simulation and experimental tests, we finally obtain the available groups of membership functions and fuzzy rules, as shown in Fig. 15.

We can obtain the ratio of the actual inertia to the original inertia $\delta = \hat{J}/J_n$ by the estimation of inertia. The inertia ratio δ is used as the input of the fuzzy inference engine, while $\triangle a_m$

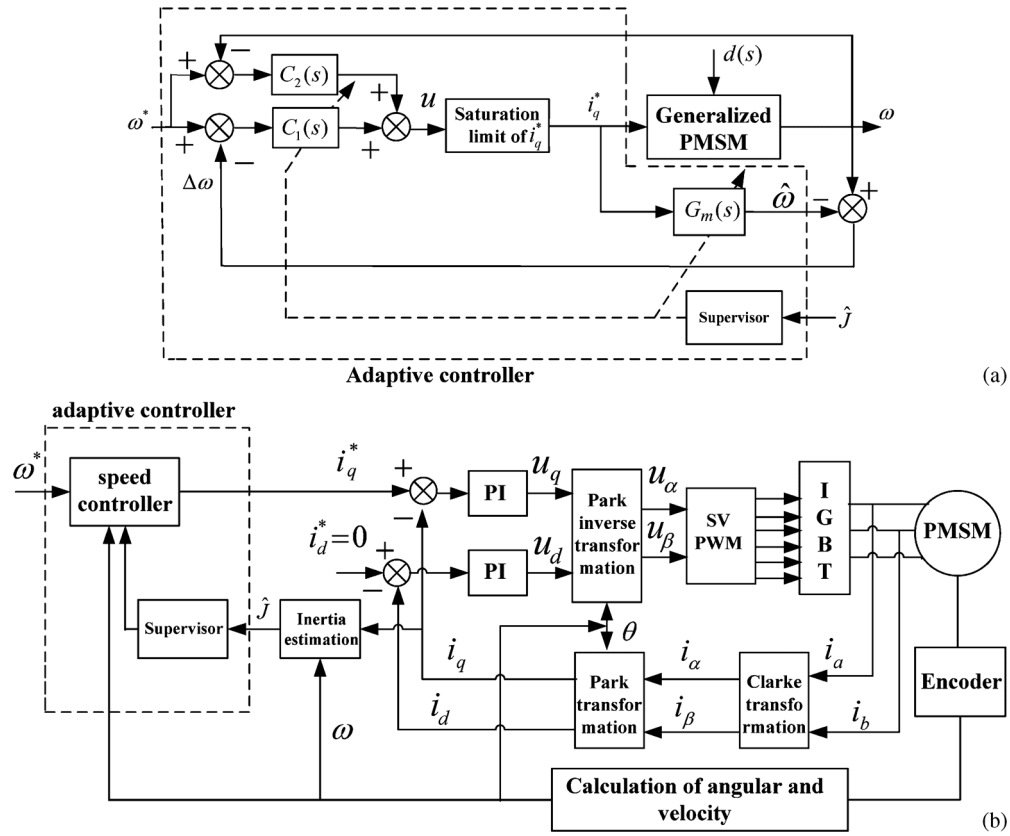

Fig. 14. Adaptive control scheme for PMSM speed regulation system. (a) The whole schematic diagram. (b) The detail diagram of adaptive IMC.

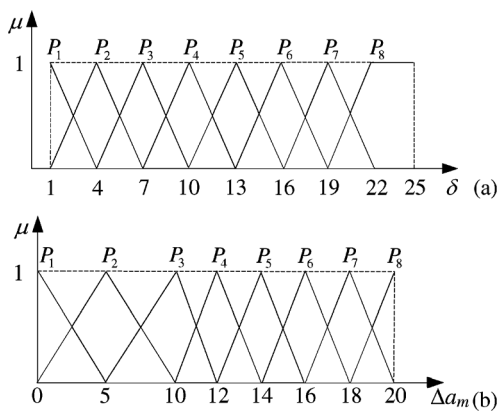

Fig. 15. Membership functions. (a) Membership function of inertia ratio δ. (b) Membership function of $\triangle a_m$.

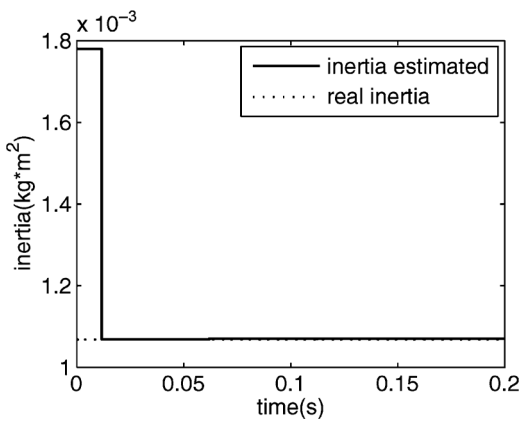

Fig. 16. Identification of inertia (solid line) and real inertia (dashed line) (simulation).

is utilized as the output of the fuzzy inference engine. The final parameter after fuzzy tuning can be expressed as follows:

$$\hat{a}_m = a_m + \gamma \triangle a_m \tag{14}$$

where γ is the proportional factor.

Here, we assume that the range of the ratio $\delta = \hat{J}/J_n$ of inertia is (0, 25]. Then, the fuzzy set of δ can be chosen as $P_1, P_2, P_3, P_4, P_5, P_6, P_7, P_8$. The fuzzy set of $\triangle a_m$ can also be chosen as $P_1, P_2, P_3, P_4, P_5, P_6, P_7, P_8$. The range of the ratio $\triangle a_m$ of is (0, 20]. The membership functions of the two fuzzy sets are shown in Fig. 15. The fuzzy inference rules are as follows: If δ is P_i, then $\triangle a_m$ is P_i $(i = 1, 2, 3 \ldots 8)$. In this paper, we use a Mamdani-type fuzzy inference engine and obtain $\triangle a_m$ by using the center of gravity method. Using (12), the parameter $\hat{a}_m$ is decided after fuzzy inference.

IV. Simulation and Experimental Results

The specification of the PMSM and other parameters of simulation are the same as Section III-A3. To test the inertia, the speed command signal is chosen as $\omega^* = 500 + 100\sin(40\pi t)$, $\gamma = 1.107 \times 10^{-4}$.

Fig. 16 is the simulation result of inertia identification when the inertia of system is increased to $6J_n$. The dashed line is

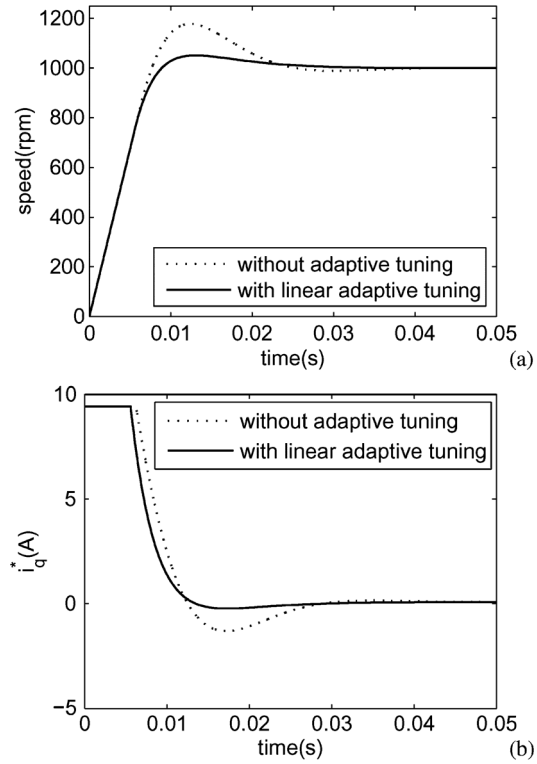

Fig. 17. Responses under linear adaptive control law and nonadaptive control law (simulation). (a) Speed. (b) i_q^*.

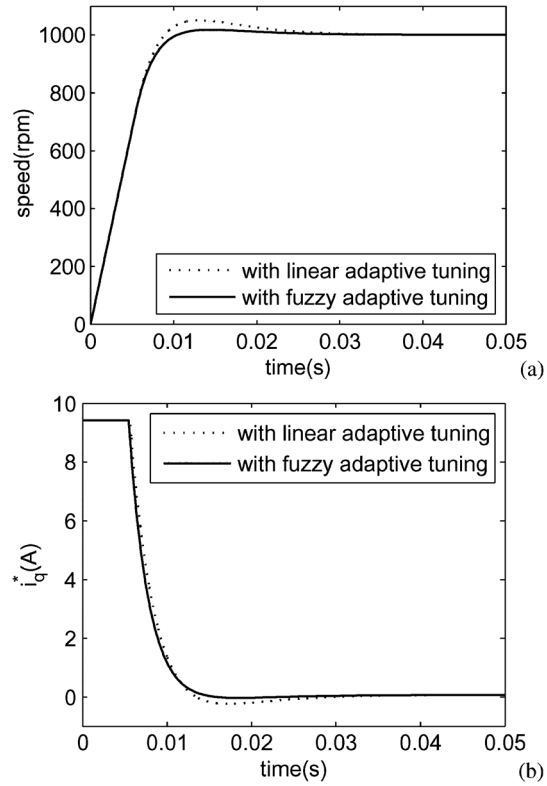

Fig. 18. Responses under linear adaptive control law and fuzzy adaptive control law (simulation). (a) Speed. (b) i_q^*.

real inertia. After inertia identification, the ratio of inertia is obtained, i.e., $\delta = 6$. According to (11), $\hat{a}_m = 6.642 \times 10^{-4}$. The speed response before and after parameter autotuning is shown in Fig. 17. Compared with the speed response without adaptive tuning (17.81% overshoot and 0.023 s settling time), the speed response under adaptive linear parameter tuning has a smaller overshoot (5.12%) and a shorter settling time (0.021 s).

In the same case, assuming that after inertia identification, the ratio of inertia is obtained, i.e., $\delta = 6$. For the fuzzy adaptive law, according to the fuzzy rule and fuzzy inference, the output of the fuzzy inference engine is $\triangle a_m = 6.98$, thus $\hat{a}_m = 8.834 \times 10^{-4}$. Fig. 18 shows the comparisons under linear adaptive tuning and fuzzy adaptive tuning. Compared with the speed response with linear adaptive tuning (5.12% overshoot and 0.021 s settling time), the speed response under fuzzy adaptive tuning has a smaller overshoot (2.12%) and a shorter settling time (0.015 s).

A. Experimental Results

To evaluate the performance of the proposed method, an experimental setup system for the speed control of a PMSM is built. The configuration and experimental test setup are shown in Figs. 19 and 20, respectively. All of the speed control algorithms, including the SVPWM technique, are implemented by the program of the DSP TMS320F2808 with a clock frequency of 100 MHz, using a C-program. The speed and current loop sampling periods are 250 and 60 μs, respectively. The saturation limit of the q-axis reference current is ± 9.42 A. The PMSM is driven by a three-phase PWM inverter with an intelligent power module with a switching frequency of 10 kHz. The

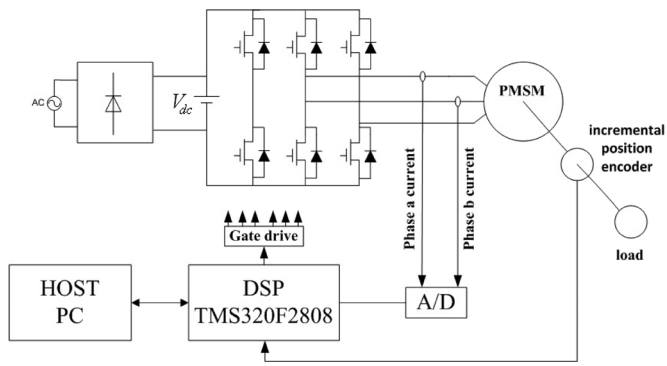

Fig. 19. Configuration of experimental system.

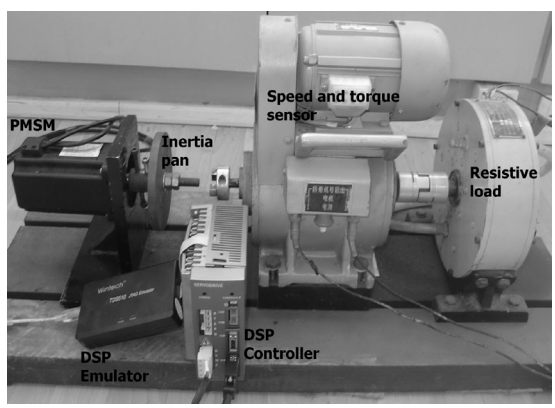

Fig. 20. Experimental test setup.

phase currents are measured by Hall-effect devices and are converted through two 12-bit A/D converters. An incremental po-

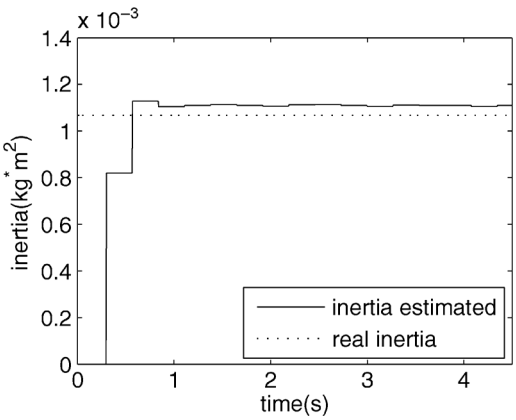

Fig. 21. Identification of inertia (solid line) and real inertia (dashed line) (experiment).

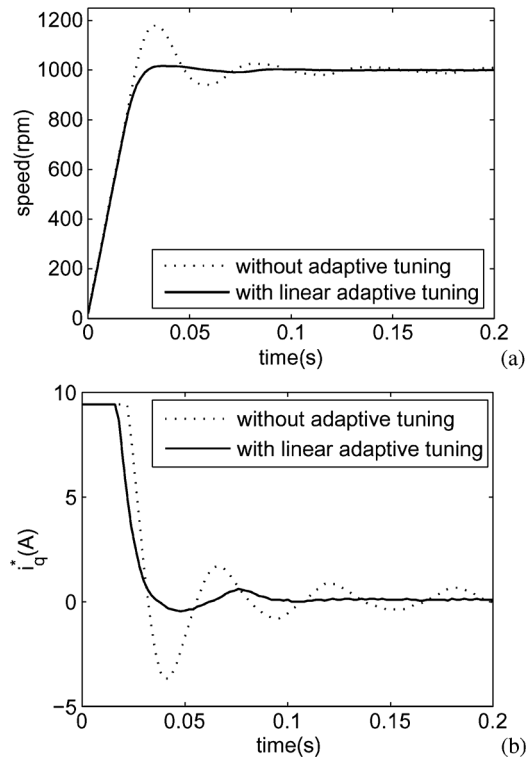

Fig. 22. Responses under linear adaptive control law and nonadaptive control law. (a) Speed. (b) i_q^*.

sition encoder of 2500 lines is used to measure the rotor speed and absolute rotor position.

The specification of the PMSM and the parameters of experiments are the same as Section III-A3. To test the inertia, the speed command signal is chosen as $\omega^* = 500 + 90\sin(5.5\pi t)$. Different specially designed mechanical inertia pans can be selected to attach to the motor so that the inertia of whole system is increased to different times of J_n. In this experiment, four kinds of inertia pans, which are about 5, 10, 15, 20 times of J_n respectively, are used to help us decide the fuzzy tuning implementation for the parameter $\hat{a}_m$ and verify the performance of the proposed adaptive control scheme.

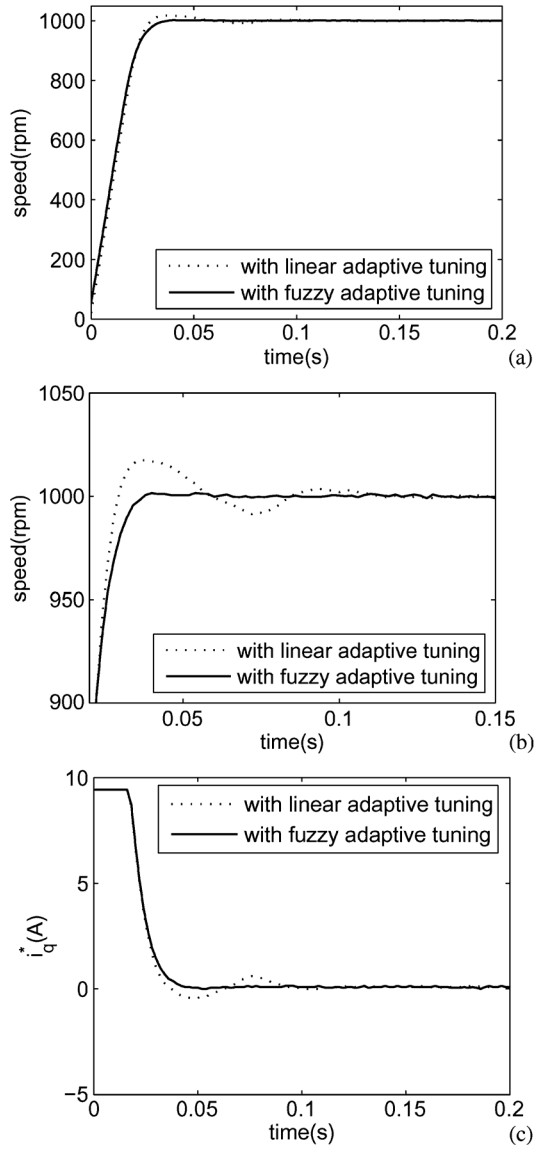

Fig. 23. Responses under linear adaptive control law and fuzzy adaptive control law. (a) Speed. (b)Local curve of (a). (c) i_q^*.

Fig. 21 shows the experimental result of inertia identification when the inertia of system is added to $6J_n$. Note that a small estimation error between the estimated inertia and the real inertia has little influence on the final control effect, since our adaptive control scheme does not need to be sensitive to the variations of inertia.

After inertia identification, the ratio of inertia is obtained, i.e., $\delta = 6$. According to (11), $\hat{a}_m = 6.75 \times 10^{-4}$. The speed response before and after parameter autotuning is shown in Fig. 22. Compared with the speed response without adaptive tuning (18.1% overshoot and 0.09 s settling time), the speed response under linear adaptive parameter tuning has a smaller overshoot (1.75%) and a shorter settling time (0.026 s).

For the same case of inertia variation, according to the fuzzy rule and fuzzy inference, the output of the fuzzy inference engine is $\triangle a_m = 6.98$, Thus $\hat{a}_m = 8.976 \times 10^{-4}$. Fig. 23 shows the comparisons under linear adaptive tuning and fuzzy adaptive tuning. Fig. 23(b) is a partial enlargement graph of Fig. 23(a).

Compared with the speed response with linear adaptive tuning (1.75% overshoot and 0.026 s settling time), the speed response under fuzzy adaptive tuning has almost no overshoot and a little longer settling time (0.03 s).

From these simulation and experimental results, it can be concluded that the speed controller with parameter autotuning possesses a good adaptation and much better dynamic performance against inertia variations.

V. Conclusion

The speed regulation problem for a permanent magnet synchronous motor (PMSM) based on internal model control methods has been studied. First, a standard internal model control scheme has been designed based on a first order model of PMSM by analyzing the relationship between reference quadrature axis current and speed output. Second, since the standard IMC method is sensitive to control input saturation and may lead to poor tracking and disturbance rejection performances, a modified internal model control scheme has been developed based on a two-port internal model control method. Third, considering the case of large variations of load inertia, two adaptive IMC schemes with two different adaptive laws have been proposed. A method based on DOB has been adopted to identify the inertia of the PMSM and load. A linear adaptive law has been developed by analyzing the relationship between the internal model and identified inertia. Considering the control input saturation in practical applications, a fuzzy adaptive law based IMC scheme has been developed based on *a priori* experimental tests and experiences, where a fuzzy inferencer based supervisor has been designed to automatically tune the parameter of speed controller according to the identified inertia. The effectiveness of the proposed methods have been verified by simulation and experimental results.

References

[1] Y. X. Su, C. H. Zheng, and B. Y. Duan, "Automatic disturbances rejection controller for precise motion control of permanent-magnet synchronous motors," *IEEE Trans. Ind. Electron.*, vol. 52, no. 3, pp. 814–823, Mar. 2005.

[2] K. H. Kim and M.-J. Youn, "A nonlinear speed control for a PM synchronous motor using a simple disturbance estimation technique," *IEEE Trans. Ind. Electron.*, vol. 49, no. 3, pp. 524–535, Mar. 2002.

[3] I. C. Baik, K.-H. Kim, and M. J. Youn, "Robust nonlinear speed control of PM synchronous motor using boundary layer integral sliding mode control technique," *IEEE Trans. Control Syst. Technol.*, vol. 8, no. 1, pp. 47–54, Jan. 2000.

[4] S. H. Li and Z. G. Liu, "Adaptive speed control for permanent magnet synchronous motor system with variations of load inertia," *IEEE Trans. Ind. Electron.*, vol. 56, no. 8, pp. 3050–3059, Aug. 2009.

[5] Y. A.-R. I. Mohamed, "Design and implementation of a robust current control scheme for a PMSM vector drive with a simple adaptive disturbance observer," *IEEE Trans. Ind. Electron.*, vol. 54, no. 4, pp. 1981–1988, Apr. 2007.

[6] S. M. Yang and Y. J. Deng, "Observer-based inertia identification for autotuning servo motor drivers," in *Proc. 40th IAS Annu. Meeting*, Hong Kong, 2005, pp. 968–972.

[7] H. H. Choi, N. T.-T. Vu, and J.-W. Jung, "Digital implementation of an adaptive speed regulator for a PMSM," *IEEE Trans. Power Electron.*, vol. 26, no. 1, pp. 3–8, Feb. 2011.

[8] F. F. M. El-Sousy, "Hybrid H-infinity-based wavelet-neural-network tracking control for permanent-magnet synchronous motor servo drives," *IEEE Trans. Ind. Electron.*, vol. 57, no. 9, pp. 3157–3166, Sep. 2010.

[9] T. L. Hsien, Y. Y. Sun, and M. C. Tsai, " $H\infty$ control for a sensorless permanent-magnet synchronous drive," *IEE Proc.-Electr. Power Appl.*, vol. 144, no. 3, pp. 173–181, 1997.

[10] Y. Luo, Y. Q. Chen, H.-S. Ahnc, and Y. G. Pi, "Fractional order robust control for cogging effect compensation in PMSM position servo systems: Stability analysis and experiments," *Contr. Eng. Practice*, vol. 18, no. 9, pp. 1022–1036, 2010.

[11] K. H. Kim, I. C. Baik, G.-W. Moon, and M.-J. Youn, "A current control for a permanent magnet synchronous motor with a simple disturbance estimation scheme," *IEEE Trans. Control Syst. Technol.*, vol. 7, no. 5, pp. 630–633, May 1999.

[12] S. H. Li, H. X. Liu, and S. H. Ding, "A speed control for a PMSM using finite-time feedback control and disturbance compensation," *Tran. Inst. Measur. Contr.*, vol. 32, no. 2, pp. 170–187, 2010.

[13] P. Cortes, M. P. Kazmierkowski, R. M. Kennel, D. E. Quevedo, and J. Rodriguez, "Predictive control in power electronics and drives," *IEEE Trans. Ind. Electron.*, vol. 55, no. 12, pp. 4312–4324, Dec. 2008.

[14] H. X. Liu and S. H. Li, "Speed control for PMSM servo system using predictive functional control and extended state observer," *IEEE Trans. Ind. Electron.*, vol. 59, no. 2, pp. 1171–1183, Feb. 2012.

[15] Y. S. Kung and M. H. Tsai, "FPGA-based speed control IC for PMSM drive with adaptive fuzzy control," *IEEE Trans. Power Electron.*, vol. 22, no. 6, pp. 2476–2486, Dec. 2007.

[16] F. J. Lin and C. H. Lin, "A permanent magnet synchronous motor servo drives using self-constructing fuzzy neural network controller," *IEEE Trans. Energy Convers.*, vol. 19, no. 1, pp. 66–72, Jan. 2003.

[17] C. E. Garcia and M. Morari, "Intenal model control-1: A unifying review and some new results," *Ind. Eng. Chem. Process Des. Develop.*, vol. 21, no. 2, pp. 308–323, 1982.

[18] C. E. Garcia and M. Morari, "Intenal model control-2: Design procedure for multivariable systems," *Ind. Eng. Chem. Process Des. Develop.*, vol. 24, no. 3, pp. 427–484, 1985.

[19] M. Morari and E. Zafirious*, Robust Process Control*. Englewood Cliffs, NJ: Prentice-Hall, 1989.

[20] I. Rivals and Z. L. Personna, "Nonlinear internal model control using neural networks: Application to process with delay and design issues," *IEEE Trans. Neural Netw.*, vol. 11, no. 1, pp. 80–90, Feb. 2000.

[21] W. F. Xie and A. B. Rad, "Fuzzy adaptive internal model control," *IEEE Trans. Ind. Electron.*, vol. 47, no. 1, pp. 193–202, Jan. 2000.

[22] Q. Zhang and E. A. Zafiriou, "A local form of small gain theorem and analysis of feedback Volterra systems," *IEEE Trans. Autom. Control*, vol. 44, no. 3, pp. 635–640, Mar. 1994.

[23] L. Harnefors and H. P. Nee, "Model-based current control of AC machines using the internal model control method," *IEEE Trans. Ind. Appl.*, vol. 34, no. 1, pp. 133–141, Jan. 1998.

[24] X. Shao, J. Zhang, Z. Zhao, and X. Wen, "Adaptive internal model control of permanent magnet synchorous motor driver system," in *Proc. 8th Int. Conf. Electr. Mach. Syst.*, Nanjing, China, 2005, vol. 3, pp. 1843–1846.

[25] I. G. Horn, J. R. Arulandu, and R. D. Braatz, "Improved filter design in internal model control," *Ind. Eng. Chem. Res.*, vol. 35, no. 10, pp. 3437–3441, 1996.

[26] T. Liu and F. Gao, "New insight into internal model control filter design for load disturbance rejection," *Contr. Theory Appl.*, vol. 4, no. 3, pp. 448–460, 2010.

[27] Q. Hu and G. P. Rangaiah, "Anti-windup schemes for uncertain nonlinear system," *IEE Proc.-Contr. Theory Appl.*, vol. 147, pp. 321–329, 2000.

[28] A. Zheng, M. V. Kothare, and M. Morari, "Anti-windup design for internal model control," *Int. J. Contr.*, vol. 60, no. 5, pp. 1015–1024, 1994.

[29] G. Stephanopoulos and H. P. Huang, "The 2-port control system," *Chem. Eng. Sci.*, vol. 41, no. 6, pp. 1611–1630, 1986.

[30] A. Datta and J. Ochoa, "A daptive internal model control design and stablity analysis," *Automatic*, vol. 32, no. 2, pp. 261–266, 1996.

[31] P. C. Krause*, Analysis of Electric Machinery*, 2nd ed. New York: McGraw-Hill, 1995.

[32] C. Eric, "Internal model predictive control," *Automatica*, vol. 31, no. 10, pp. 1471–1482, 1995.

[33] I. Awaya, Y. Kato, I. Miyake, and M. Ito, "New motion control with inertia identification function using disturbance observer," in *Proc. Power Electron. Motion Control Conf*, San Diego, CA, 1992, pp. 77–81.

[34] J. W. Choi, S. C. Lee, and H. G. Kim, "Inertia identification algorithm for high-performance speed control of electric motors," *Proc. Inst. Elect. Eng.-Electr. Power Appl.*, vol. 153, no. 3, pp. 379–386, May 2006.

[35] B. Kosko, *NN and Fuzzy System: A Dynamical Systems Approach to Machine Intelligence*. Englewood Cliffs, NJ: Prentice-Hall, 1992.
[36] L. Zadeh, "Outline of a new approach to the analysis of complex systems and decision processes," *IEEE Trans. Syst.. Man, Cybern*, vol. 3, no. 1, pp. 28–44, Jan. 1973.

Shihua Li (M'05–SM'10) was born in Pingxiang, Jiangxi Province, China. in 1975. He received the B.Sc., M.Sc., and Ph.D. degrees from Southeast University, Nanjing, China, in 1995, 1998 and 2001, respectively, all in automatic control.

Since 2001, he has been with School of Automation, Southeast University, where he is currently a Professor. His main research interests include nonlinear control theory with applications to robots, spacecraft, AC motors, and other mechanical systems.

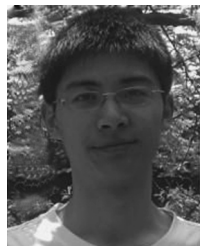

Hao Gu was born in Changzhou, Jiangsu Province, China, in 1985. He received the B.Sc. degree in automatic control from Hohai University, Nanjing, China, in 2008, and the M.Sc. degree in automation from Southeast University, Nanjing, China, in 2011.

Since 2011, he has been with Huawei Technologies Company, Ltd., Nanjing, China.